1 **An Equation to Line the Borders of Folding-Unfolding Transition Diagram of Lysozyme**

2

3 Mohammad Amin Mohammad,*[†,‡] Ian M. Grimsey[†], and Robert T. Forbes[†,§]

4 [†]Drug Delivery Group, School of Pharmacy, University of Bradford, Bradford BD7 1DP, UK.

5 [‡]Department of Pharmaceutics, Faculty of Pharmacy, University of Damascus, Damascus, Syria.

6 [§]School of Pharmacy and Biological Sciences, University of Central Lancashire, PR12HE, UK.

7

8 * Corresponding author
9 Dr Mohammad Amin Mohammad
10 Associate Professor in Pharmaceutical Technology
11 First name: Mohammad Amin
12 Family name: Mohammad
13 Phone: + 44 (0)1225 386797
14 Email: mam2014uk@gmail.com
15 Postal address: Dr. Mohammad Amin Mohammad, School of Pharmacy, University of Bradford,
16 Bradford, West Yorkshire, BD7 1DP, UK.
17
18 Dr Ian M. Grimsey
19 Senior Lecturer in Pharmaceutical Technology
20 Phone: +44 (0)1274 234754
21 Fax: +44 (0)1274 234769
22 i.m.grimsey@bradford.ac.uk
23 School of Pharmacy
24 University of Bradford
25 Bradford, West Yorkshire, BD7 1DP.
26
27 Prof Robert T. Forbes
28 Professor of Clinical Pharmaceutics
29 Phone: +44 (0)1772 893513
30 rtforbes@uclan.ac.uk
31 School of Pharmacy and Biomedical Sciences
32 University of Central Lancashire
33 Preston, Lancashire, PR1 2HE.
34
35
36
37
38
39

40    **ABSTRACT**

41

42    It is important for the formulators of biopharmaceuticals to predict the folding-unfolding

43    transition of proteins. This enables them to process proteins at predetermined conditions without

44    denaturation. Depending on apparent denaturation temperature ($T_m$) of lysozyme, we have

45    derived an equation describing its folding-unfolding transition diagram. According to water

46    content and temperature, this diagram was divided into three different areas which are the area of

47    the water-folded lysozyme phase, the area of the water-folded lysozyme phase and the bulk

48    water phase, and the area of the denatured lysozyme phase. The amount of water content

49    controlled the appearance and intensity of Raman band at ~1787 cm$^{-1}$ when lysozyme powders

50    were thermally denatured at temperatures higher than $T_m$.

51

52

53

54

55

56

57

58

59

60

61

62

## INTRODUCTION

Protein structure and dynamics are determined by the intraprotein and protein-water non-covalent interactions.[1,2] Hydration degree of proteins, which is the weight ratio of water to protein, should be ~0.2 to initiate protein function, moreover, full protein function requires a hydration degree of ~1.[3] However, proteins are in their solid state during pharmaceutical processes and storage. Water contents of protein powders affect their stability and performance.[4] Water content alters the mechanisms of proteins' degradation reactions, and this alteration also depends on other conditions such as temperature and the formulation compositions.[5] In general, increasing water content decreases the stability of protein powders. Water acts as a plasticizer which enhances the molecular mobility of the proteins and so leads to an increase in their degradation rates. This shortens the shelf-life of solid protein powders and formulations.

Many studies have used lysozyme as a model protein to understand the effect of the water content on protein stability using differential scanning calorimetry (DSC). Previous works used sealed DSC pans to study the effect of water content on the glass transition temperature ($T_g$) of lysozyme, they found that $T_g$ of lysozyme decreased by increasing the water content to approach a plateau level.[6,7] Similarly, increasing water content within lysozyme powders decreased their apparent denaturation temperature ($T_m$) in sealed DSC pans.[8] Therefore, both water content and temperature line the borders between the native (folded) and denatured (unfolded) states of lysozyme powders. These borders are important to predetermine the processing conditions (water content and temperature) which preserve the native structure of proteins during manufacturing processes (e.g., spray drying). Here, we derive an equation correlating water content of lysozyme powders with their $T_m s$, and then use this equation to line the borders of the folding-unfolding

86 transition diagram of lysozyme. Also, we use Raman spectroscopy to monitor water content

87 effect on the molecular conformation of lysozyme upon the thermal unfolding transition of

88 lysozyme powders.

89

90 **EXPERIMENTAL METHODS**

91

92 **Materials.** Lyophilized hen egg-white lysozyme powder (Biozyme Laboratories, UK)

93 was purchased and considered to be unprocessed lysozyme powder.

94 **Sample Preparation.** The unprocessed lysozyme powder was used to prepare a series of

95 lysozyme powders with different water contents either by raising or reducing their water content.

96 The water residues were manipulated by exposing the powders to humidified air or to anhydrous

97 nitrogen gas for different times at 30 °C. The prepared powders were immediately sealed and left

98 to equilibrate at room temperature at least for a weak after preparation. This time is enough to

99 ensure uniformity of water distribution in lysozyme particles.[9] The prepared series of lysozyme

100 powders were tested to correlate the water content with $T_m$. To monitor the water content effect

101 on the molecular conformation of lysozyme upon the thermal unfolding transition, the lysozyme

102 powders with different water contents were thermally denatured inside hermetically sealed pans

103 by heating to temperatures higher than their unfolding transition peaks. These samples were

104 considered to be the thermally denatured lysozyme powders.

105 **Thermogravimetric analysis (TGA).** The water content of each powder was determined

106 using Thermo Gravimetric Analysis (TGA) (Perkin Elmer Ltd., UK). Samples (5-10 mg) were

107 heated from 30 °C to 210 °C at a scan rate of 10 °C/min in an aluminum pan under nitrogen flow

108 at 20 ml/min. Each sample was analyzed in triplicate. The decrease in the weight before

4

109      decomposition was considered as water content. TGA results were validated by re-analyzing the

110      water content of some samples using Karl Fischer Titration (KFT) (701 KF Titrino with 703 Ti

111      stand, Metrohm, Switzerland). Using TGA instead of KFT as only a few mg is enough for TGA.

112      **Differential scanning calorimetry (DSC).** $T_m$ of each sample was measured using

113      Differential Scanning Calorimetry (DSC) (Perkin-Elmer Ltd., UK). To study the effect of water

114      residue on the thermal stability of lysozyme (the value of $T_m$), the evaporation of water during

115      heating was suppressed by using Large Volume Capsules, which are stainless steel sample

116      containers equipped with an O-ring seal to provide a hermetic seal. Lysozyme powders (5-10mg)

117      and solutions in water (20 µl) were encapsulated in the hermetically sealed pans and scanned

118      between 40 °C to 200 °C at 5 °C/min in triplicate. DSC was also used to prepare the thermally

119      denatured lysozyme powders by heating them inside the hermetically sealed pans to temperatures

120      higher than their unfolding transitions.

121      **FT-Raman spectroscopy.** FT-Raman spectra of the lysozyme powders at different water

122      content and their thermally denatured lysozyme counterpart powders were recorded with a

123      Bruker IFS66 optics system using a Bruker FRA 106 Raman module. The excitation source was

124      an Nd: YAG laser operating at 1064 nm and a laser power of 50 mW was used. The FT-Raman

125      module is equipped with a liquid nitrogen cooled germanium diode detector with an extended

126      spectrum band width covering the wave number range 1850-1100 cm$^{-1}$. Samples were placed in

127      stainless steel sample cups and scanned 200 times with the resolution set at 8 cm$^{-1}$. The observed

128      band wave numbers were calibrated against the internal laser frequency and are correct to better

129      than ±1 cm$^{-1}$. The spectra were corrected for instrument response. The experiments were run at a

130      controlled room temperature of 20 ±1°C.

131

## Results and discussion

We employed this protein because it folds in a highly cooperative manner and so exhibits an all-or-none thermal unfolding transition, and so it displayed one denaturation peak, in solid and solution states,[10,11] which makes the study easier. The driest prepared lysozyme powder contained 2.6±0.1 %w/w water and its $T_m$ was 436.9±0.6 K, while the wettest powder contained 20.3±2.3 %w/w water and its $T_m$ was 355.5±3.1 K. In Figure 1 is a DSC thermogram of each sample, showing an inverse correlation between water content and $T_m$s.
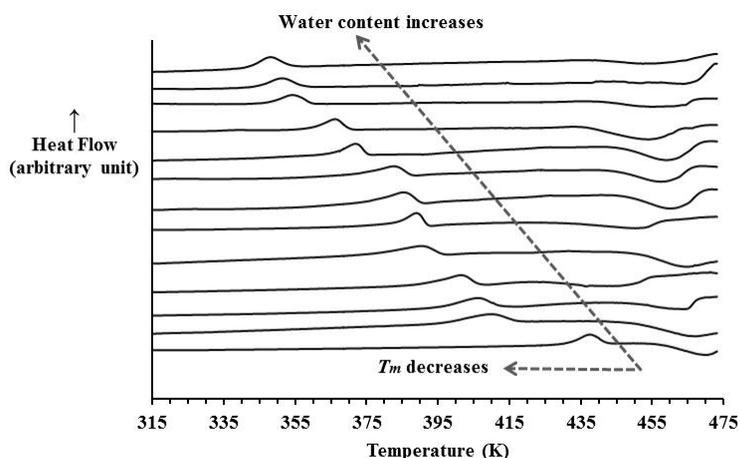


**Figure 1.** Differential scanning calorimetry thermograms of lysozyme powders (in sealed pans) at different water content.

Previous study demonstrated that DSC thermograms of lysozyme powders with different water content performed in pierced pans showed two endothermic peaks, the first broad peak, which extends from ~298 to 433 K, indicates water evaporation and its area directly correlates to the water content, the second peak at ~473 K refers to the protein denaturation ($T_m$) and its

146 position is independent of water content because water evaporates through the pierced pans

147 before the unfolding transition (denaturation) of lysozyme.[10]

148      However, unlike the experiments performed in the pierced pan, Figure 1 shows that the

149 position of the endothermic unfolding peak ($T_m$) varied for different water contents when DSC

150 experiments were performed under sealed conditions. The DSC thermograms (Figure 1) did not

151 show the water evaporation peak because the evaporation of water during heating was

152 suppressed by the hermetical seal, i.e., the pressure generated from increasing the temperature of

153 the air, which had been trapped during the capsulation of the hermetically sealed pans, prevented

154 water loss. Figure 1 also show an exothermic peak after lysozyme unfolding in all samples

155 analysed with the sealed pans. This peak was reproducible and showed little variation between

156 samples, with a peak position ranging from 453 to 468 K. It was believed that this exothermic

157 peak could be due to the aggregation of lysozyme molecules after unfolding, however re-

158 scanning the sealed pans containing previously aggregated lysozyme powders also gave an

159 exothermic peak at the same position but without the endothermic unfolding peak.

160      We hypothesized that water molecules associate with lysozyme powders to form a

161 homogenous water-folded lysozyme phase. This phase unfolds at a kinetic thermal energy

162 depending on water mole fraction ($X_w$) and lysozyme mole fraction ($X_p$) within the powders.

163 When $X_w$ increases, $T_m$ of the unfolding kinetic energy is reduced, and its reduction stops when

164 the water molecules reach their saturation limit within the water-folded lysozyme phase. Above

165 this limit, water molecules segregate from the water-folded lysozyme phase to form another

166 phase of bulk water, and so they cannot reduce $T_m$ further.

167      $X_w$ / $X_p$ equals N, the ratio of water molecules to lysozyme molecules, and it is calculated

168 according to Eq. (1):

7

169
$$N = 14296 \times W\%/18 \times P\% \qquad (1)$$

170   18 and 14296 are the molecular weights of water and lysozyme, respectively, and W% and P%

171   are the percentage of water weight and protein weight in the powders, respectively. The results

172   were tabulated in Table 1.

173

**Table 1.** The apparent denaturation temperature ($T_m$), number of water molecules associating with one lysozyme molecule ($N$), water mole fraction ($X_w$) and lysozyme mole fraction ($X_p$) of lysozyme powders at different water content.

| Water content %w/w | $T_m$ (K) | $N$ | $X_w$ | $X_p$ |
|---|---|---|---|---|
| 2.5 (0.1) | 436.9 (0.6) | 20.4 | 0.9532 | 0.0468 |
| 4.6 (0.3) | 412.0 (1.6) | 38.1 | 0.9744 | 0.0256 |
| 5.2 (0.1) | 406.2 (2.1) | 43.4 | 0.9775 | 0.0225 |
| 6.4 (0.2) | 401.9 (1.4) | 54.3 | 0.9819 | 0.0181 |
| 7.7 (0.1) | 390.3 (0.2) | 66.6 | 0.9852 | 0.0148 |
| 8.5 (0.1) | 388.8 (2.6) | 73.8 | 0.9866 | 0.0134 |
| 9.2 (0.5) | 385.5 (0.3) | 80.5 | 0.9877 | 0.0123 |
| 9.9 (0.1) | 383.5 (0.6) | 87.7 | 0.9887 | 0.0113 |
| 12.0 (0.1) | 371.8 (0.4) | 108.7 | 0.9909 | 0.0091 |
| 14.4 (0.1) | 365.7 (0.4) | 133.1 | 0.9925 | 0.0075 |
| 15.6 (0.6) | 364.0 (1.6) | 146.6 | 0.9932 | 0.0068 |
| 20.3 (2.3) | 355.5 (3.1) | 201.8 | 0.9951 | 0.0049 |

Values within parenthesis are standard deviation, n = 3.

174

175       $T_m$ reflects the value of thermal kinetic energy needed to overcome the cohesion energy

176   stabilizing the folded state of proteins. This cohesion energy results from Van der Waals

177   attraction, electrostatic interaction, hydrogen bonding, and conformational entropy (hydrophobic

178   effect).[12] Electrostatic and hydrophobic interactions play the main roles in protein folding.[1,13]

179   Water affects these interactions and hence the magnitude of $T_m$ needed to unfold proteins. Water

180   molecules surround the surface of protein molecules and penetrate into their cavities.[14]

181   Surrounding water molecules strengthen the hydrophobic effect by an increase in the entropy of

182   water due to association between hydrophobic residues.[13] However, according to Coulomb's law,

183   the interior waters weaken the electrostatic forces because they increase the dielectric constant in

184   the interior of protein molecules and also increase the distances between polarized and ionized

185   groups of proteins.[15,16] Our results demonstrated that the net effect of water weakens the forces

186   responsible for the folded state, and so the increased water content facilitates the protein

187   unfolding at lower $T_m$. Dehydration of lysozyme powders stabilizes its native form because the

188   free energy change of the lysozyme denaturation increases by dehydration.[17]

189       Multiplying the gas constant ($R$) by $T_m$ gives the kinetic thermal energy needed to unfold

190   lysozyme. Interestingly, our data (Table 1) prove that $RT_m$ and $\ln N$ correlate linearly with a

191   correlation coefficient close to one (r = $-0.997$), and their linear equation is:

192   $$\ln N = \text{Slope } RT_m + \text{Intercept} \qquad (2)$$

193   Figure 2 shows the straight line of Eq. (2) which was regressed in Eq. (3).

194   $$\ln N = -\frac{RT_m}{72.3} + 15.0 \qquad (3)$$

195   where 72.3 has units of Cal.mole$^{-1}$ and 15.0 has units of mole.mole$^{-1}$ (i.e., unitless). $R$ =

196   1.9872041 Cal.mole$^{-1}$.K$^{-1}$, therefore Eq. (3) can be reduced to Eq. (4):

197   $$T_m = -36.4 \ln N + 545.7 \qquad (4)$$
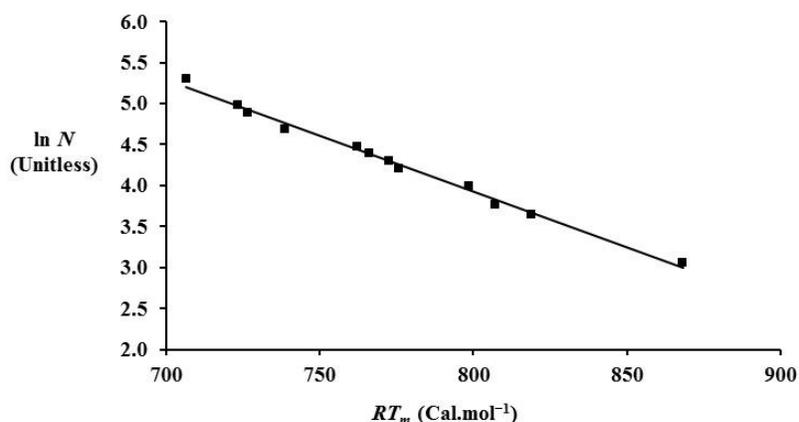
198



**Figure 2.** The linear correlation between the denaturation thermal kinetic energy and logarithm of water molecules associating with one lysozyme molecule.

199       We measured $T_m$s of lysozyme solutions containing 80 %w/w and 70 %w/w of water.

200    $T_m$s of the solutions were 348.2±0.7 and 348.0±1.0 K, respectively, and they were similar (T-

201    test: P < 0.05). According to our hypothesis, $T_m$ of the lysozyme solutions equals the apparent

202    denaturation temperature of the saturated water-lysozyme phase ($T_m^S$). Therefore, we extrapolated

203    Eq. (4) to $T_m^S$ (348K), which is the same as that of the solutions, to calculate the number of water

204    molecules which saturate one molecule of lysozyme ($N^S$) as follows:

205    $$T_m^S = -36.4 \ln N^S + 545.7 \qquad (5)$$

206    The calculated $N^S$ was 228 water molecules according to Eq. (5). This water amount is

207    equivalent to 22.3 %w/w and 0.3 g/g protein. We then prepared another lysozyme powder with a

208    water content of 23.2±1.1 %w/w, which is similar to the calculated $N^S$. $T_m$ of the prepared water

209    saturated powder was 347.8±1.4 K, which is similar to $T_m^S$ (T-test: P < 0.05). Therefore, we used

210    temperature and N to draw the folding-unfolding transition diagram of lysozyme. Figure 3 shows

211    this diagram in which the denaturation line obeys Eq. (3) until reaching the water saturated solid

212    state at $N^S$. After this value of water molecules, $T_m$ did not significantly change. Our calculated

213    value of $N^S$, i.e. 228 water molecules, is similar to previously reported values of the hydration

214    shell of lysozyme. Previous researchers used gigahertz to terahertz spectroscopy[18,19] Raman

215    spectroscopy[20] neutron and X-ray scattering[21] NMR[22] to quantitate the hydration shell of

216    lysozyme, and these methods estimated similar values of the hydration shell of lysozyme, and the

217    values ranged between 170-270 water molecules. Hydration shell molecules have different

218    properties from bulk water.[23] Our results demonstrate that the effect of water molecules on $T_m$

219    changed at $N > N^S$. Therefore, we speculate that water molecules begin to form the bulk water at

220    $N > N^S$. Therefore, the folding-unfolding transition diagram of lysozyme (As shown in Figure 3)

221    was divided to three areas; (A) represents the area of the water-folded lysozyme phase, (B)

222   represents the area of the water-folded lysozyme phase and the bulk water phase, and (C)

223   represents the area of the denatured lysozyme phase, and the line separating (C) form (A) and

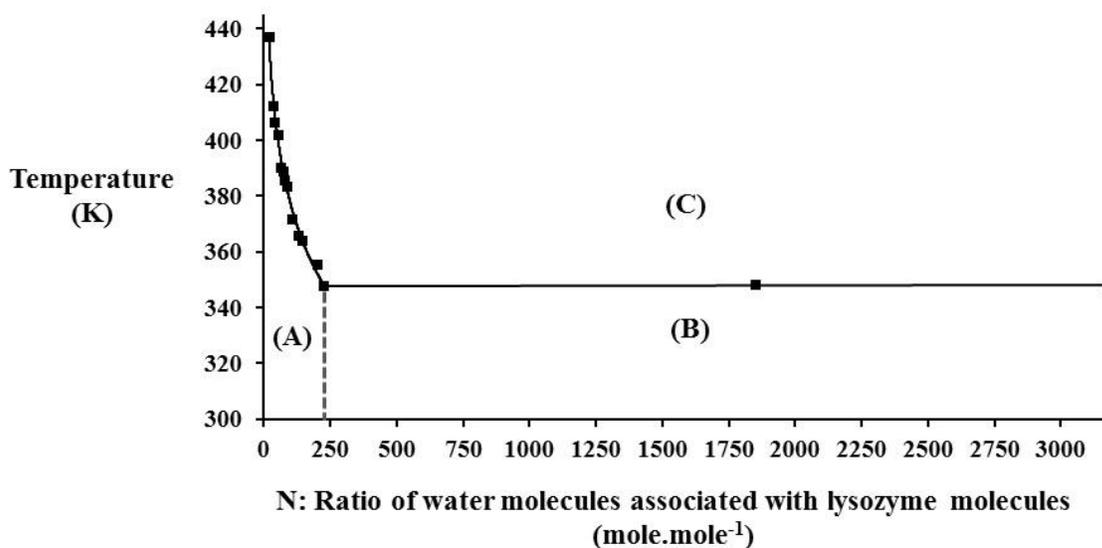224   (B) is the denaturation line.

225   



**Figure 3.** The folding-unfolding transition diagram of lysozyme. (A) represents the area of the water-folded lysozyme phase, (B) represents the area of the water-folded lysozyme phase and the bulk water phase, and (C) represents the area of the denatured lysozyme phase; the line separating (C) form (A) and (B) is the denaturation line.

226   

227   Although $T_m$ of lysozyme solutions is usually ~348 K, it changes due to additives (e.g.,

228   co-solvents, pH, ionic strength).[10,24,25] Also, additives changed $T_m$ of lysozyme powders.[8] We

229   could conclude that if the additives are miscible with water, they will participate in forming

230   water-protein phases (in both solid and solution states). Therefore, they would change the

231   constants of Eqs. (3) and (5). Whilst other proteins may have different constants.

232   Previous Raman study clarified the significant effects of hydration degree of native

233   lysozyme powders on the back bone and the side chain conformations of lysozyme.[9] In other

234   words, this previous study covered the molecular conformation of lysozyme under the

235 denaturation line of the folding-unfolding transition diagram of lysozyme. Here, the molecular

236 conformation of lysozyme above the denaturation line were investigated. Raman spectra of the

237 thermally denatured powders at different hydration degree and their original powders were

238 collected at room temperature and presented in Figure 4. The peak intensities of the spectra were

239 normalized using the band at 1447 cm$^{-1}$ (CH bending) as internal intensity standard. This is

240 because its intensity and position are unaffected by changes induced in protein structure after
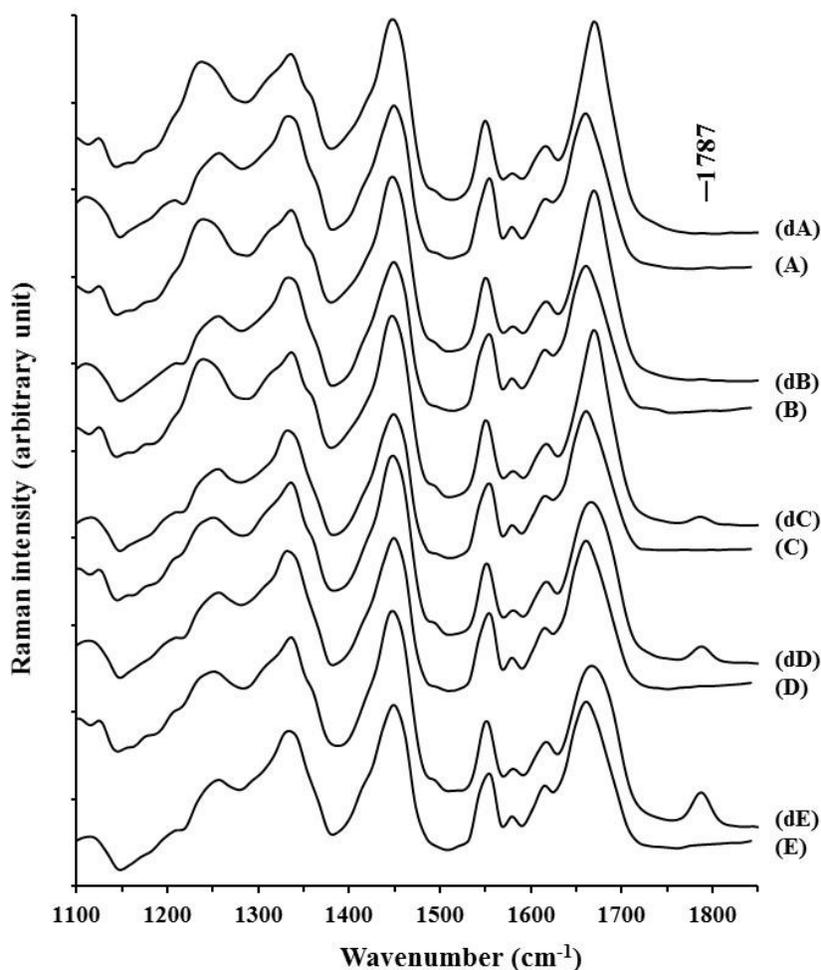
241 applying different stresses.[26]

242



**Figure 4.** Representative Raman spectra of lysozyme powders in the 1100−1850 cm$^{-1}$ wavenumber region, (A), (B), (C), (D) and (E) represent lysozyme powders at different water content of 20.3, 12.0, 8.2, 5.2 and 2.5 %w/w, respectively, and (dA), (dB), (dC), (dD) and (dE)

represent their thermally denatured counterpart powders (in sealed pans), respectively.

243    Within the investigated wavenumber region (1100−1850 cm$^{-1}$), we did not notice

244    significant differences between the studied original lysozyme samples (Figure 4, spectra A, B, C,

245    D and E). However, compared to the original lysozyme powders, the Raman spectra of the

246    counterpart thermally denatured powders showed changes in the the peak positions of amide I

247    and amide III bands. The peak of amide I was upshifted from ~1660 to ~1671 cm$^{-1}$ after thermal

248    denaturation (Figure 4, spectra dA, dB, dC, dD and dE), and also spectra dD and dE show

249    broadening in the amide I band in the case of the thermally denatured samples at low hydration

250    degree (5.2 and 2.5 %w/w). The peak of amide III was downshifted from ~1256 to ~1249 cm$^{-1}$ at

251    low hydration degree (spectra dD and dE), and it was further downshift to ~1240 cm$^{-1}$ with an

252    increase in the intensity at higher hydration degree (spectra dA, dB and dC). The Raman Bands

253    of the amide I (C=O stretch) and amide III (N-H in-plane bend + C-N stretch) are indicators of

254    the protein's secondary structures.[9] The mid-point of amide I is expected to be at 1665±5 cm$^{-1}$

255    for α-helix and 1670±3 cm$^{-1}$ for β-sheet and disordered secondary structure, and the mid-point of

256    amide III is expected to be at 1267±8 cm$^{-1}$ for α-helix, 1235±5 cm$^{-1}$ for β-sheet and 1245±4 cm$^{-1}$

257    for disordered structure.[27,28] Therefore, the changes in Raman bands (presented in Figure 4)

258    indicate that the content of the β-sheet and disordered secondary structure were increased and at

259    the same time the α-helix content was decreased after the thermal denaturation. Similar changes

260    in the positions of amide I and amide III Raman bands of lysozyme powders were reported when

261    lysozyme powders were denatured using mechanical stress[10] and γ-radiation[29], and the

262    researchers attributed these changes to a decrease in the α-helix with an increase in the β-sheet

263    and disordered structures. However, in the case of the thermally denatured powders, a new

264    Raman band at ~1787 cm$^{-1}$ appeared, and its intensity decreased by raising the water content

13

265    (Figure 4, spectra dC, dD and dE), and the peak disappeared at water content $\geq$ 12 %w/w (Figure

266    4, spectra dA and dB). Therefore, the appearance of this peak at 1787 cm$^{-1}$ relates to the nature

267    of lysozyme molecules' movement during the thermal unfolding transition and this movement

268    depends heavily on the amount of hydration degree of the powders. The new band at 1787 cm$^{-1}$

269    could be assigned to the stretching of free hydrogen bonding carbonyl group. As the line of

270    amide I at wavenumbers $\geq$ 1685 cm$^{-1}$ is expected to be assigned to the disordered secondary

271    structure without hydrogen bonding.[27] It can be concluded that the higher the water content in

272    lysozyme powders during unfolding transition, the higher the freedom for lysozyme molecules to

273    move and saturate the free carbonyl groups of the peptide bonds resulted from the unfolding

274    transition. At water content $\geq$ 12 %w/w, the lysozyme molecules have enough freedom to move

275    and saturated all the free carbonyl groups, and this explains the disappearance of the Raman band

276    at 1787 cm$^{-1}$. This finding agrees with previous results stating that at water content between 11

277    and 21 %w/w, lysozyme possess a glasslike dynamic transition from rigid to flexible state due to

278    the mobility increase of the structural units.[30]

279          Therefore, the shape of amide I Raman band, the position and intensity of amide III

280    Raman band, and the intensity of the Raman band at ~1787 cm$^{-1}$ of the thermally denatured

281    powders depend on the water content of their original native powders. This indicates that the

282    molecular structure of the thermally denature lysozyme depends on its hydration degree.

283          This folding-unfolding transition diagram of lysozyme was obtained using sealed pans in

284    order to ensure mass conservation of the water-lysozyme system. Therefore, it was determined at

285    constant volume but variable pressure. Fortunately, in our case, we capsulated the sealed pans at

286    atmospheric pressure (~0.1MPa), and according to the general gas law, the increase in the

287    pressure due to the temperature increase from 298 to 473 K inside the hermetically sealed pans

288 would reach ~0.2 MPa. This pressure values have a negligible role in the lysozyme denaturation.

289 It was confirmed that lysozyme is denatured when pressure is at much higher values >500

290 MPa.[31]

291

292 **CONCLUSIONS**

293

294     These results allowed us to derive an equation correlating $T_m$ of lysozyme with its

295 hydration degree. $T_m$ exponentially decreased when the hydration degree increased, and it did

296 not significantly decrease further after hydration degree reaching a value similar to hydration

297 shell of the lysozyme. We used the derived equation to draw the folding-unfolding transition

298 diagram of lysozyme. This diagram will be useful to process lysozyme at predetermined

299 conditions of temperature and water content without denaturation. The molecular conformation

300 of the thermally denatured lysozyme was found to be dependent on the hydration degree of the

301 original native powders. A new Raman band at 1787 cm^{-1} appeared in the spectra of the

302 thermally denatured lysozyme, and its intensity reversibly correlated with the water content and

303 it disappeared at the water content $\geq$ 12 %w/w.

304

305 **AUTHOR INFORMATION**

306 Corresponding Author

307 *E-mail: mam2014uk@gmail.com

308 Notes

310

311

## ACKNOWLEDGEMENTS

313

317

**REFERENCES**

(1) Ji, C.; Mei, Y. Some practical approaches to treating electrostatic polarization of proteins. *Acc. Chem. Res.* 2014, *47*, 2795–2803.

(2) Dhindsa, G. K.; Tyagi, M.; Chu, X. Q. Temperature-dependent dynamics of dry and hydrated beta-casein studied by quasielastic neutron scattering. *J. Phys. Chem. B* 2014, *118*, 10821–10829.

(3) Frauenfelder, H.; Chen, G.; Berendzen, J.; Fenimore, P. W.; Jansson, H.; McMahon, B. H.; Stroe, I. R.; Swenson, J.; Young, R. D. A unified model of protein dynamics. *Proc. Natl. Acad. Sci. U.S.A.* 2009, *106*, 5129–5134.

(4) Broadhead, J.; Rouan, S. K.; Hau, I.; Rhodes, C. T. The effect of process and formulation variables on the properties of spray-dried beta-galactosidase. *J. Pharmacol. Pharmacother.* 1994, *46*, 458–467.

(5) Wang, W. Lyophilization and development of solid protein pharmaceuticals. *Int. J. Pharm.* 2000, *203*, 1–60.

(6) Miyazaki, Y.; Matsuo, T.; Suga, H. Low-temperature heat capacity and glassy behavior of lysozyme crystal. *J. Phys. Chem. B* 2000, *104*, 8044–8052.

(7) Panagopoulou, A.; Kyritsis, A.; Aravantinou, A. M.; Nanopoulos, D.; Serra, R. S. I.; Ribelles, J. L. G.; Shinyashiki, N.; Pissis, P. Glass transition and dynamics in lysozyme-water mixtures over wide ranges of composition. *Food Biophys.* 2011, *6*, 199–209.

(8) Bell, L. N.; Hageman, M. J.; Muraoka, L. M. Thermally induced denaturation of lyophilized bovine somatotropin and lysozyme as impacted by moisture and excipients. *J. Pharm. Sci.* 1995, *84*, 707–712.

(9) Kocherbitov, V.; Latynis, J.; Misiunas, A.; Barauskas, J.; Niaura, G. Hydration of lysozyme studied by Raman spectroscopy. *J. Phys. Chem. B* 2013, *117*, 4981−4992.

(10) Mohammad, M. A.; Grimsey, I. M.; Forbes, R. T. Mapping the solid-state properties of crystalline lysozyme during pharmaceutical unit-operations. *J. Pharm. Biomed. Anal.* 2015, *114*, 176–183.

(11) Maroufi, B.; Ranjbar, B.; Khajeh, K.; Naderi-Manesh, H.; Yaghoubi, H. Structural studies of hen egg-white lysozyme dimer: comparison with monomer. *Biochim. Biophys. Acta* 2008, *1784*, 1043–1049.

(12) Yano, Y. F. Kinetics of protein unfolding at interfaces. *J. Phys. Condens. Matter* 2012, *24*, 503101–503117.

350 (13) Wu, Z.; Cui, Q.; Yethiraj, A. Driving force for the association of hydrophobic peptides: the
351 importance of electrostatic interactions in coarse-grained water models. *J. Phys. Chem. Lett.*
352 2011, *2*, 1794–1798.
353 (14) Tilton, R. F. Jr.; Kuntz, I. D. Jr.; Petsko, G. A. Cavities in proteins: Structure of a
354 metmyoglobin xenon complex solved to 1.9 .ANG. *Biochemistry* 1984, *23*, 2849–2857.
355 (15) Dwyer, J. J.; Gittis, A. G.; Karp, D. A.; Lattman, E. E.; Spencer, D. S.; Stites, W. E.;
356 García-Moreno E, B. High apparent dielectric constants in the interior of a protein reflect water
357 penetration. *Biophys. J.* 2000, *79*, 1610–1620.
358 (16) Pitera, J. W.; Falta, M.; Van Gunsteren, W. F. Dielectric properties of proteins from
359 simulation: the effects of solvent, ligands, pH, and temperature. *Biophys. J.* 2001, *80*, 2546-2555.
360 (17) Kocherbitov, V.; Arnebrant, T. Hydration of thermally denatured lysozyme studied by
361 sorption calorimetry and differential scanning calorimetry. *J. Phys. Chem. B* 2006, *110*, 10144–
362 10150.
363 (18) Vinh, N. Q.; Allen, S. J.; Plaxco, K. W. Dielectric spectroscopy of proteins as a quantitative
364 experimental test of computational models of their low-frequency harmonic motions. *J. Am.*
365 *Chem. Soc.* 2011, *133*, 8942–8947.
366 (19) Knab, J.; Chen, J. Y.; Markelz, A. Hydration dependence of conformational dielectric
367 relaxation of lysozyme. *Biophys. J.* 2006, *90*, 2576–2581.
368 (20) Bellavia, G.; Paccou, L.; Achir, S.; Guinet, Y.; Siepmann, J.; Hédoux, A. Analysis of Bulk
369 and Hydration Water During Thermal Lysozyme Denaturation Using Raman Scattering. *Food*
370 *Biophys.* 2013, *8*, 170–176.
371 (21) Svergun, D. I.; Richard, S.; Koch, M. H. J.; Sayers, Z.; Kuprin, S.; Zaccai, G. Protein
372 hydration in solution: experimental observation by x-ray and neutron scattering. *Proc. Natl.*
373 *Acad. Sci. U.S.A.* 1998, *95*, 2267–2272.
374 (22) Kuntz, I. D. Hydration of macromolecules. III. Hydration of polypeptides. *J. Am. Chem.*
375 *Soc.* 1971, *93*, 514–516.
376 (23) Choudhuri, J. R.; Chandra, A. An ab initio molecular dynamics study of the hydrogen
377 bonded structure, dynamics and vibrational spectral diffusion of water in the ion hydration shell
378 of a superoxide ion. *Chem. Phys.* 2014, *445*, 105–112.
379 (24) Blumlein, A.; McManus, J. J. Reversible and non-reversible thermal denaturation of
380 lysozyme with varying pH at low ionic strength. *Biochim. Biophys. Acta. Proteins and*
381 *Proteomics* 2013, *1834*, 2064–2070.
382 (25) Chen, P.; Seabrook, S. A.; Epa, V. C.; Kurabayashi, K.; Barnard, A.S.; Winkler, D. A.;
383 Kirby, J. K.; Ke, P. C. Contrasting effects of nanoparticle binding on protein denaturation. *J.*
384 *Phys. Chem. C* 2014, *118*, 22069–22078.
385 (26) Yu, T. J.; Lippert, J. L.; Peticolas, W. L. Laser Raman studies of conformational variations
386 of poly-L-lysine. *Biopolymers* 1973, *12*, 2161−2176.
387 (27) Li-Chan, E. C. Y. The applications of Raman spectroscopy in food science.
388 *Trends. Food. Sci. Tech.* 1996, *7*, 361-370.
389 (28) Yu, N. T.; Liu, C. S. Laser Raman Spectra of Crystalline and Aqueous Glucagon. *J. AM.*
390 *Chem. Soc.* 1972, *94*, 5127-5135.
391 (29) Torreggiani, A.; Tamba, M.; Manco, I.; Faraone-Mennella, M. R.; Ferreri, C.;
392 Chatgilialoglu, C. Radiation damage of lysozyme in a biomimetic model: some insights by
393 Raman spectroscopy. *J. Mol. Struct.* 2005, *744*, 767−773.
394 (30) Kocherbitov, V.; Arnebrant, T.; Söderman, O. Lysozyme−water interactions studied by
395 sorption calorimetry. *J. Phys. Chem. B* 2004, *108*, 19036−19042.

396  (31) Hédoux, A.; Guinet, Y.; Paccou, L. Analysis of the mechanism of lysozyme pressure
397  denaturation from Raman spectroscopy investigations, and comparison with thermal
398  denaturation. *J. Phys. Chem. B* 2011, *115*, 6740–6748.

399  **TOC GRAPHICS**

$$T_m = -36.4 \ln N + 545.7 \text{ when } N \leq N^S$$

$$T_m \cong T_m^S \text{ when } N \geq N^S$$

$T_m$: Apparent denaturation temperature
of lysozyme.

N: Ratio of water molecules to lysozyme
molecules.

S: Superscript refers to saturated
water-lysozyme state.

400